Passive Safety Design of a Gen-IV Reactor with MOX Fuel and Sodium Coolant

Matéo Bellouard, Faisal Ahmed Moshiur, Jeevan George

July 13, 2023

Abstract

This report presents the design and analysis of a passively safe Generation IV nuclear reactor with MOX fuel and sodium coolant. The design parameters include a coolant temperature increase of 100 K from the inlet to the outlet of the core, a fraction of nominal power to be removed by natural convection of 0.10, a dip-cooler elevation of 20.0 m, and a fuel height of 1.0 m with a peak burnup of 10%. The cladding tube is required to survive a transient temperature of 1000 K for 200 s, with a 5% Am fraction. The rod diameter and pitch are calculated using a peak channel power of 5 kW. Meanwhile, the fuel composition yielding a minimum reactivity swing for a burnup of 6% is identified using SERPENT. The critical mass and number of fuel rods are also determined, and the configuration's conversion ratio and minor actinide burning rate are calculated. Reactivity coefficients are determined at the beginning of life. This report demonstrates the feasibility of a passively safe Gen-IV reactor with MOX fuel and sodium coolant and provides valuable insight into its design and operation.

Keywords: *passively safe, Gen-IV reactor, MOX fuel, sodium coolant, natural convection, dip-cooler, burnup, cladding tube, transient temperature, SERPENT, reactivity swing, critical mass, conversion ratio, minor actinide burning rate, reactivity coefficients.*

1 Introduction

Nuclear energy has long been recognized as a viable alternative to conventional fossil fuels for power generation. However, nuclear safety and waste management concerns have led to development of advanced reactor designs that offer improved safety and efficiency. Generation IV (Gen-IV) nuclear reactors are among the most promising of these designs, offering enhanced safety features and reduced waste production. This report presents the design and analysis of a passively safe Gen-IV reactor with MOX fuel and sodium coolant. The reactor design parameters are based on specific requirements for coolant temperature increase, natural convection, dip-cooler elevation, fuel height and burnup, and cladding tube survival. Using computational tools such as SERPENT [7], we investigate key performance metrics such as criticality, reactivity coefficients, and minor actinides behavior in the reactor setup. This report demonstrates the feasibility of a passively safe Gen-IV reactor design with MOX fuel and sodium coolant and provides valuable insights into its design and performance.

2 Design and Parameters

From the previous assignment, we took the speed of coolant at the nominal condition as 8 m/s when the

temperature of the coolant is 820 K [3].

In transient conditions, both oxide and metallic alloy fuels have the potential to release all the fission gases they contain into the gas space within the rod. Therefore for 100% Xe and He releases from the fuel, with an Am fraction of 5% ensuring the cladding tube can survive a transient temperature (T_c) of 1000 K for 200 s (t_r), the pressure of fission gas, P_{FG}, can be used to calculate plenum elevation [4].

$$P_{FG} = \frac{n_{FG} \times R_{FG} \times T_{FG}}{V_{plenum}} \tag{1}$$

where, n_{FG} is number of fission gas atoms, R_{FG} is the gas constant, T_{FG} is the fission gas temperature and V_{plenum} is the plenum volume.

From Eq. (1), the pressure of fission gas, P_{FG}, can be rewritten as

$$P_{FG} = \frac{\rho_{fuel}}{M_{fuel}} \times R_{FG} \times T_{FG} \times BU_{FIMA} \times Y_{FG} \times \frac{V_{fuel}}{V_{plenum}}, \tag{2}$$

where V_{fuel} is the fuel volume,

$$n_{FG} = n_{A_n} \times Y_{FG} \times BU_{FIMA},$$

and the number density of actinides in a solid fuel are taken as $\frac{n_{A_n}}{V_{fuel}} = \frac{\rho_{fuel}}{M_{fuel}}$ [4]. The Xenon and Krypton atom production, Y_{FG}, is taken as 25% per fission, and BU_{FIMA} is the burnup FIMA. Burnup (FIMA) stands for "Fission per Initial Metal Atom." It is a measure used to quantify the amount of fission that has occurred in a nuclear fuel material. For this project, our objective is to find a fuel composition that results in the smallest change in reactivity when the burnup reaches 6% of Fission per Initial Metal Atom (FIMA).

Experimental data indicates that the time it takes for rupture to occur in $15-15$Ti material can be described using a parameterization Eq. (3) [4], specifically,

$$P = 21100 - 1.89 \times 10^{-6}\sigma_{hoop} - 0.030 \times 10^{-12}\sigma_{hoop}^2, \tag{3}$$

when the hoop stress is within the range of 100 to 400 MPa. Moreover, the time to creep rupture of a cladding tube can be used to calculate the Larson-Miller parameter, P, as shown in Eq. (4) [4].

$$P = T_c(17.6 + \log_{10}(t_r)) \tag{4}$$

where time for rupture, t_r, is expressed in hours, and the temperature of the cladding tube, T_c, in Kelvin.

The released gas causes hoop stress on the cladding tube.

$$\sigma_{hoop} \simeq \frac{\bar{r}_{clad}}{\delta_{clad}} P_{FG} \tag{5}$$

where $\bar{r}_{clad}$ is the average cladding radius and δ_{clad} is the cladding thickness [4].

From Eq. (2), the plenum volume can be written as

$$V_{plenum} = \frac{\rho_{fuel}}{M_{fuel}} \times R_{FG} \times T_{FG} \times BU_{FIMA} \times Y_{FG} \times \frac{V_{fuel}}{\sigma_{hoop}^{max}} \frac{\bar{r}_{clad}}{\delta_{clad}} \tag{6}$$

where σ_{hoop}^{max} is the maximum hoop stress on the cladding tube caused by the released gas.

Therefore, we can get this expression of plenum elevation, H_{plenum}, from the Eq. (6)

$$H_{plenum} = \frac{\rho_{fuel}}{M_{fuel}} \times R_{FG} \times T_{FG} \times BU_{FIMA} \times Y_{FG} \times \frac{H_{fuel}}{\sigma_{hoop}^{max}} \frac{\bar{r}_{clad}}{\delta_{clad}}. \tag{7}$$

Since the sum of fuel height and plenum of height gives the value of fuel channel height, we found the channel height for our design from the postulated value of fuel elevation of 1 m (as shown in Tab. 1) by adding it with the value of H_{plenum} obtained using Eq. (7).

The hydraulic diameter, D_h, can be linked to the pressure loss, ΔP_{nom}, caused by friction during nominal and natural flow circumstances [4].

$$\Delta P_{nom} = |\alpha_{Na}| \times g \times \Delta T \times H_{DC} \times \left(\kappa \frac{\dot{Q}_{nom}}{\dot{Q}_{res}}\right)^{(2-b)}, \tag{8}$$

and

$$D_h \approx \left(\frac{a \times K}{2} \frac{H_{ch}}{\Delta P_{nom}}\right)^{\frac{1}{(1+b)}} \left(\rho_{Na}^{1-b} v_{nom}^{2-b} \mu_{Na}^{b}\right)^{\frac{1}{(1+b)}}, \tag{9}$$

where $\kappa = 1.0$ is the factor of increase in $\Delta T = 100$ K for the coolant from inlet to outlet of the core during transient and a fraction of nominal power to be removed by natural convection of 0.10, so $\frac{\dot{Q}_{nom}}{\dot{Q}_{res}} =$

$\frac{1}{0.10}$, $g = 9.81$ m/s^2 is the gravitational acceleration, $H_{DC} = 20.0$ m for the elevation of dip-coolers, and $a = 0.485$ & $b = 0.29$ are empirical parameters found in wire spaced channels under nominal and natural convection conditions [4]. Moreover, $\alpha_{coolant}$, $\mu_{coolant}$ and $\rho_{coolant}$ are Doppler coefficient, viscosity and density respectively. These are coolant physical properties dependent on temperature. In the context of this report, the coolant chosen for the simulation and design is sodium, so we have used these relations provided by ANL and NEA [1]:

$$\mu_{Na}(T) = \frac{e^{-6.4406+\frac{556.835}{T}}}{T^{0.3958}} \tag{10}$$

$$\rho_{Na}(T) = 219 + 275.32\left(1 - \frac{T}{2503.7}\right) + 511.58\left(1 - \frac{T}{2503.7}\right)^{\frac{1}{2}} \tag{11}$$

The thermal expansion coefficient, α_{Na}, is the change of density with temperature, $\alpha_{Na} \equiv \frac{d\rho_{Na}}{dT}$ [5]. Therefore, the simplified form of its expression for sodium coolant is

$$\alpha_{Na}(T) = -0.2205 - 3.846\times10^{-5}T + 1.691\times10^{-8}T^2. \tag{12}$$

The mass flow rate is calculated from the relation below [9],

$$\dot{m} = \frac{\dot{Q}^{peak}_{channel}}{\Delta T \times c_{P,Na}} \tag{13}$$

where $c_{P,Na}$ is the specific heat capacity of sodium as a coolant dependent on temperature, and

$$\dot{Q}^{peak}_{channel} = \chi^{peak}_{fuel} \times \frac{H_{fuel}}{2} = 5 \text{ kW} \tag{14}$$

where χ^{peak}_{fuel} is the peak linear power density of the fuel and H_{fuel} is the fuel elevation [4].

The suggested correlation for determining the specific heat capacity is as follows[1]:

$$c_{P,Na}(T) = 1658.2 - 0.849T + 4.4541\times10^{-4}T^2 - \frac{2.9926\times10^6}{T^2}. \tag{15}$$

The hexagonal fuel channel geometry as a simplified triangular lattice is shown in Fig. 1.

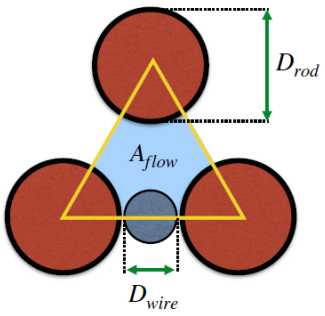

Figure 1: Hexagonal fuel channel geometry with wire spacer [4].

The flow area of the coolant, A_{flow}, can be calculated from Eq. (13) [9]

$$A_{flow} = \frac{\dot{m}}{\rho_{Na} \times v_{nom}}. \tag{16}$$

By using Eq. (16), we can get expressions for rod radius and spacer wire radius for an assembly channel [4], as shown below:

$$r_{rod} = \frac{2}{\pi}\left(\frac{A_{flow}}{D_h} + \sqrt{\left(\frac{A_{flow}}{D_h}\right)^2\left(\frac{4\sqrt{3}}{\pi} - 1\right) - \frac{\pi}{4}A_{flow}}\right), \tag{17}$$

and

$$r_{wire} = \frac{2}{\pi}\left(\frac{A_{flow}}{D_h} - \sqrt{\left(\frac{A_{flow}}{D_h}\right)^2\left(\frac{4\sqrt{3}}{\pi} - 1\right) - \frac{\pi}{4}A_{flow}}\right). \tag{18}$$

Now using Eq. (17) and Eq. (18), the pitch of the assembly can be evaluated as depicted below [4]:

$$P = 2r_{rod} + 2r_{wire} \tag{19}$$

Using the equations above, along with the given input parameters, we have determined the geometry of our reactor. The results are presented in Tab. 1.

3 Results and Discussion

3.1 Reactivity Swing

From the instructions, our fuel had to have a constant Americium fraction of 5%. The remaining had to be

Table 1: Parameters obtained from given constraints.

Parameter	Value
Temperature	**820** K [3]
$\mathbf{v_{nom}}$	**8.0** m/s [3]
Hydraulic diameter	1.35 mm
Mass flow rate	0.0397 kg/s
Flow area	6.05×10^{-2} cm^2
Rod radius	**5.68** mm
Wire radius	0.0430 mm
Pitch	**11.4** mm
P/D	**1.01**
MOX density	10.9 g/cm^3
M_{fuel}	272 g/mol
$P_{rupture}$	1.63×10^4 MPa
H_{fuel}	1.0 m [4]
H_{plenum}	0.226 m
$\mathbf{H_{ch}}$	**1.23** m

split between Plutonium and Uranium, and the ideal composition corresponded to the one for which we obtained the smaller reactivity swing. The reactivity swing was calculated for different fuel compositions by changing the concentration of Pu in the mix from 9% to 15%. After several fuel optimization calculations, we found the mix's minimum reactivity swing at a concentration of 14.25% Pu. Fig. 2 to 5 show the effective multiplication factors versus the Burnup rate for the fuel compositions used. If the Plutonium fraction is too small, the multiplication factor will increase with increasing burnup, while we will observe the inverse trend with too much Plutonium. Our aim was thus to find the concentration of Plutonium at the tipping point where the trend changes its behavior and for which we have the smallest reactivity swing. Fig. 6 shows the fuel composition where the reactivity swing is minimal, at a concentration of 14.3%. From the article on the discrepancy between Burnup FIMA and Specific Burnup,[2], we found that for MOX fuels at 6% BU_{FIMA}, the Burnup is approximately 57 MWd/kgHM. From this optimization, we obtained the fuel composition we used for our fuel, and the molar proportions are listed in Tab. 2.

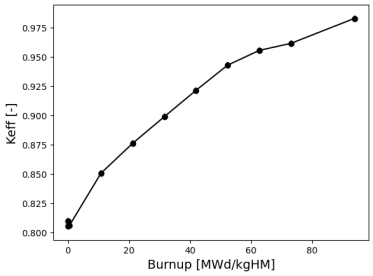

Figure 2: Effective multiplication factor at 9% Pu.

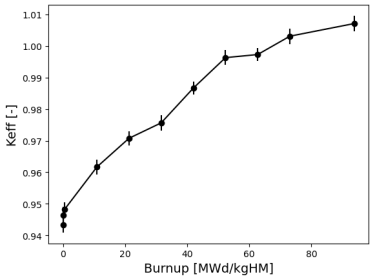

Figure 3: Effective multiplication factor at 12% Pu.

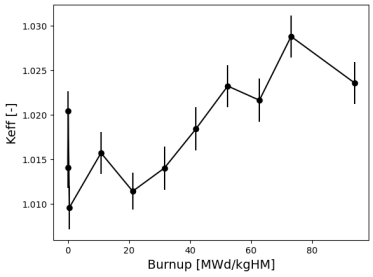

Figure 4: Effective multiplication factor at 13.5% Pu.

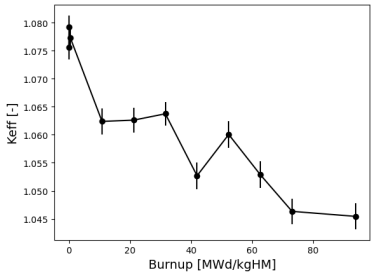

Figure 5: Effective multiplication factor at 15% Pu.

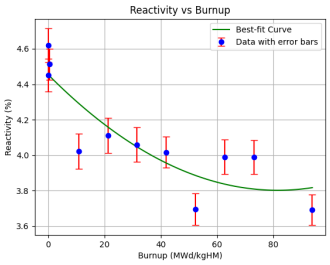

Figure 6: Reactivity Swing at 14.3% Pu.

Table 2: Composition of the Fuel

Isotopes	Composition
U238	0.8075
Pu238	0.004987
Pu239	0.073957
Pu240	0.033915
Pu241	0.018382
Pu242	0.011257
Am241	0.02500
Am243	0.02500

3.2 Critical configuration

From the previous section, we have been able to determine the optimal composition of the fuel, and using this and the geometry of our reactor, we determined the critical configuration of the reactor. The critical configuration was obtained by removing several assemblies in the reactor until the mean reactivity obtained with the SERPENT was as close as possible to the criticality, i.e., $k_{eff} \approx 1$. This has been obtained with the geometry shown in 7. From this, we extracted the number of fuel rods by counting the number of fuel assemblies in the reactor and knowing that each of our assemblies was made of a 13 by 13 hexagonal lattice full of fuel rods. The critical mass has been obtained first by extracting the fuel volume using the serpent command "sss2 -checkvolumes" and multiplying this value by the fuel density. The results are compiled in Tab. 3.

Table 3: Critical configuration of the reactor

Critical Mass (Tons)	40.743
Number of Fuel assemblies	309
Number of rods	52221

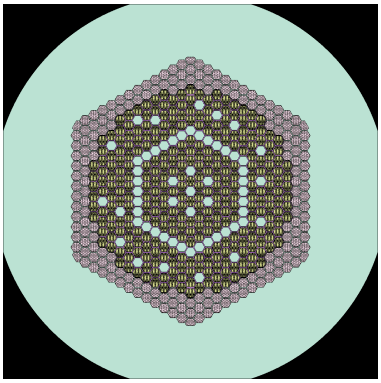

Figure 7: Configuration for which the reactor was critical

3.3 Minor actinide burning rate

What we understood for this part was to track the trend of the different isotopes of the main minor actinides: americium and curium. The evolution is shown in Fig. 8. We can observe that with increasing burnup, the americium densities will decrease as expected as they will turn into other actinides, especially ^{244}Cm, for which we observe the most significant increase in density.

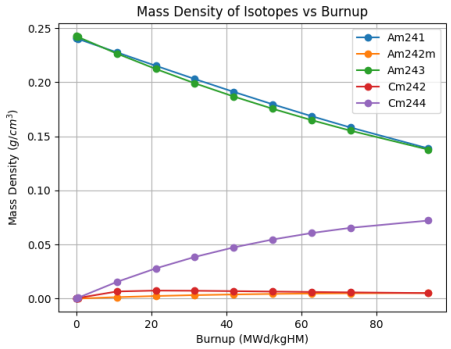

Figure 8: Evolution of the mass density of Am and Cm isotopes as a function of burnup

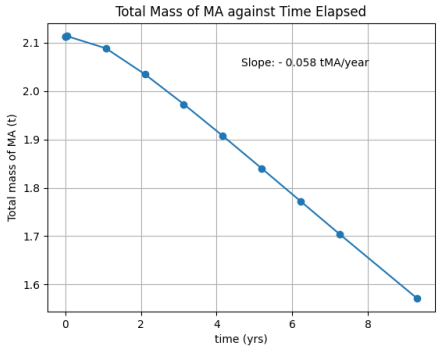

Figure 9: Time evolution of the total mass of minor actinides

Minor actinides burning rate found from linear regression [8] plot from the depletion data obtained from SERPENT simulation, i.e., the total mass of the minor actinides is plotted against the time elapsed to see the trend of decrease in minor actinides from Fig. 9.

3.4 Conversion Ratio

To compute the conversion ratio, we used the formula given in the lecture notes [6] :

$$CR_{ip} = \frac{\Sigma_{A,m}\sigma_c(^mA)C(^mA)\eta(^{m+1}A'))}{\Sigma_{A,m}\sigma_f(^mA)C(^mA)\eta(^mA)} \tag{20}$$

And we ran our input file on SERPENT, adding detectors to compute the cross-sections in our configuration. From this we obtained a value $CR_{ip} = \mathbf{1.076}$. This value is over 1, as expected for a Gen IV reactor, but still pretty close to 1, which can be explained by our MOX fuel and should give small conversion ratio values.

3.5 Reactivity coefficients

At the beginning of life, we calculated two reactivity coefficients for our reactor: the Doppler coefficient and the Coolant temperature feedback. The Doppler coefficient, α_D, was computed using the Doppler constant, K_D, defined as:

$$\alpha_D = \frac{K_D}{T_f} \tag{21}$$

where T_f is the fuel temperature and the Doppler constant is given below from

$$K_D = \frac{\rho(T_1) - \rho(T_2)}{\ln\left(\frac{T_2}{T_1}\right)}. \tag{22}$$

The coolant temperature feedback was calculated as

$$\alpha_{coolant} = \frac{\Delta\rho}{\Delta T} \tag{23}$$

.

When the temperature of the fuel increases, the fuel rods will be dilated a bit, so the height of the fuel rods will increase, decreasing the fuel density and increasing the neutron leakage. To compute the effect of the axial expansion of the fuel, we increased the height of the fuel rod by 5% and decreased the fuel density accordingly to study the reactivity change. Then we used the same kind of equation as for α_C:

$$\alpha_{axial} = \frac{\Delta\rho}{\Delta T} \tag{24}$$

.

The diagrid radial expansion coefficient comes from the increase in the size of the diagrid, which holds the fuel assemblies when the temperature increases. Consequently, the distance between the fuel assemblies will affect the reactivity, and we proceeded the

same way, increasing this distance by 5% and observing the change in reactivity. Again, the formula used to compute the diagrid radial expansion is:

$$\alpha_{diagrid} = \frac{\Delta\rho}{\Delta T} \tag{25}$$

.

Table 4: Reactivity Coefficients

Coefficients	Values
K_D	-457 ± 50.0 pcm
α_D	-0.427 ± 0.005 pcm/K
$\alpha_{coolant}$	0.453 ± 0.199 pcm/K
α_{axial}	-0.259 ± 0.050 pcm/K
$\alpha_{diagrid}$	-0.920 ± 0.120 pcm/K

We simulated several temperatures for each coefficient and obtained the values presented in Tab. 4.

References

[1] J. K. Fink and L. Leibowitz. *Thermodynamic and Transport Properties of Sodium Liquid and Vapor*. Technical Report ANL/RE-95/2. Argonne, IL: Argonne National Laboratory, 1995. URL: https://www.osti.gov/biblio/83436.

[2] J. Cetnar G. Kepisty. *On the discrepancies between FIMA and Specific Burnup*. Technical Report. 2017.

[3] Janne Wallenius. *Gen IV reactors course, Home assignment 3*. Course assignment. Course code: SH2613. 2023. URL: https://canvas.kth.se/courses/37978/files/6340579/download?download_frd=1.

[4] Janne Wallenius. *Gen IV reactors course, Lecture: Design a Gen-IV reactor for passive safety*. Course lecture. Course code: SH2613. 2023. URL: https://canvas.kth.se/courses/37978/files/6501018/download?download_frd=1.

[5] Janne Wallenius. *Gen IV reactors course, Lecture: Minor actinide burning*. Course lecture. Course code: SH2613. 2023. URL: https://canvas.kth.se/courses/37978/files/6374917/download?download_frd=1.

[6] Janne Wallenius. *Gen IV reactors course, Physics of breeding*. Course lecture. Course code: SH2613. 2023. URL: https://canvas.kth.se/courses/37978/files/6269059?module_item_id=628835.

[7] Jaakko Leppänen. *Serpent – a Continuous-energy Monte Carlo Reactor Physics Burnup Calculation Code*. VTT Technical Research Centre of Finland. VTT Science 71. 2014. URL: https://www.vtt.fi/inf/pdf/science/2014/S71.pdf.

[8] F. Pedregosa et al. *Scikit-learn: Machine Learning in Python*. Software. 2011. DOI: 10.5281/zenodo.1213433. URL: https://scikit-learn.org/stable/index.html.

[9] J. Wallenius and S. Bortot. "Coolants for Fast Neutron Generation IV Reactors". In: *Fast Neutron Generation IV Reactors*. Ed. by M.A. Pouchon and A. Ballagny. Amsterdam, Netherlands: Elsevier, 2016. Chap. 7, pp. 153–170.